

Molecular Dynamics Simulation of Carboxy-Myoglobin Embedded in a Trehalose-Water Matrix

Grazia Cottone,^{*†} Lorenzo Cordone,[†] and Giovanni Ciccotti^{*}

^{*}INFN and Physics Department, University of Rome La Sapienza, 00185 Rome; and [†]INFN and Department of Physical and Astronomical Sciences, University of Palermo, 90123 Palermo, Italy

ABSTRACT We report on a molecular dynamics (MD) simulation of carboxy-myoglobin (MbCO) embedded in a water-trehalose system. The mean square fluctuations of protein atoms, calculated at different temperatures in the 100–300 K range, are compared with those from a previous MD simulation on an H₂O-solvated MbCO and with experimental data from Mössbauer spectroscopy and incoherent elastic neutron scattering on trehalose-coated MbCO. The results show that, for almost all the atomic classes, the amplitude of the nonharmonic motions stemming from the interconversion among the protein's conformational substates is reduced with respect to the H₂O-solvated system, and their onset is shifted toward higher temperature. Moreover, our simulation shows that, at 300 K, the heme performs confined diffusive motions as a whole, leaving the underlying harmonic vibrations unaltered.

INTRODUCTION

Trehalose is a nonreducing disaccharide (see Fig. 1) found in rather large quantities in organisms that can afford extreme conditions, such as quite high temperatures (>60°C) and lack of water, in a state of suspended animation called anhydrobiosis (Crowe and Crowe, 1984; Bianchi et al., 1991; Panek, 1995). It has been shown that trehalose protects biomolecules during dehydration, preserves their activity, and stabilizes them against the effects of adverse ambient conditions (Crowe et al., 1996). The observation that trehalose protects biostructure from heat denaturation put forward the relevance of studying the dynamics of proteins embedded in trehalose matrices. This could help in understanding up to which extent the external matrix can affect the internal dynamics of proteins and, in particular, the interconversion among conformational substates (Frauenfelder et al., 1988).

Flash photolysis experiments on carbon-monoxo myoglobin (MbCO, see Fig. 2) embedded in a trehalose glass (trehalose-coated) showed that some part of the protein dynamics is strongly inhibited (Hagen et al., 1995, 1996; Gottfried et al., 1996). In particular, the escape of CO from the heme pocket at room temperature was prevented, even after prolonged illumination. Cordone et al. (1998) reported that in trehalose-coated MbCO the protein-specific motions (defined as the nonharmonic motions arising from thermal fluctuations of a protein molecule among conformational substates (Frauenfelder et al., 1988)), detected by Mössbauer and by optical absorption spectroscopy, are significantly hindered. Moreover, the hydrogen atom mean-square displacements, measured by incoherent elastic neutron scattering,

appeared, in extremely dry MbCO samples, to be the ones of a harmonic solid even at room temperature (Cordone et al., 1999). This was confirmed by the behavior of the density of states measured by inelastic neutron scattering (Cordone et al., 1999). At variance, previous elastic neutron scattering measurements on hydrated MbCO (Doster et al., 1989), showed the appearance of nonharmonic contributions to hydrogen atom motions for $T \geq 160$ K. More recent results (Librizzi et al., 1999a, and work in progress) showed that highly localized protein-specific motions, detected from the thermal interconversion among A substates of MbCO, are progressively hindered by decreasing the sample water content. The above interconversion was barely detectable in extremely dry samples, containing only residual tightly bound water molecules. [MbCO A substates are those conformational substates corresponding to three specific environments experienced by the bound CO within the heme pocket (Vojtechovsky et al., 1999); they are reflected in the splitting to three different sub-bands of the CO stretching band (Makinen et al., 1979). Their thermal interconversion is not hindered in hydrated MbCO films (Mayer, 1994)].

Previous molecular dynamics (MD) simulations (Sakurai et al., 1997; Liu et al., 1997; Bonanno et al., 1998; Conrad and de Pablo, 1999) performed on trehalose-water systems have already demonstrated that trehalose remarkably modifies the hydrogen bond network and water dynamics. MD simulation may also provide a better understanding of the effects of trehalose coating, by exploring the internal dynamics of proteins embedded in the external sugar matrix at the molecular level. In this work we studied an MbCO molecule in a system containing 231 trehalose and 538 water molecules, using MD technique. We performed a set of simulations at different temperatures in the 100–300 K range. Information on the internal protein motions was obtained through the evaluation of the atomic mean-square fluctuations (MSFs).

Received for publication 17 March 2000 and in final form 4 October 2000.

Address reprint requests to Dr. Lorenzo Cordone, INFN and Department of Physical and Astronomical Sciences, University of Palermo, Via Archirafi 36, 90123 Palermo, Italy. Tel.: 39-091-6234215; Fax: 39-091-6162461; E-mail: cordone@fisica.unipa.it.

© 2001 by the Biophysical Society

0006-3495/01/02/931/08 \$2.00

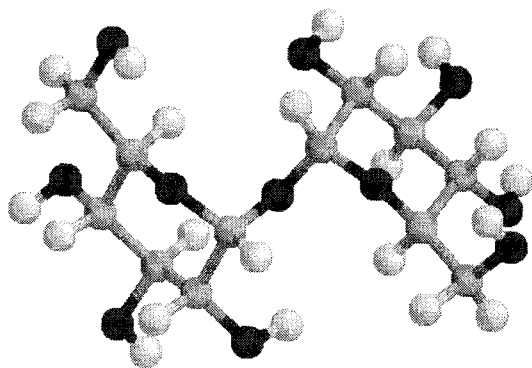


FIGURE 1 Trehalose molecule. *Black spheres*: oxygen atoms; *dark gray spheres*: carbon atoms; *light gray spheres*: hydrogen atoms.

We compared the obtained MSFs with the ones from a previous simulation on an H₂O-solvated MbCO (Venturoli, 1998) and with the experimental MSFs obtained through Mössbauer spectroscopy and neutron scattering on MbCO trehalose-coated, dry samples (Cordone et al., 1998, 1999).

The computational methods used in the simulations and in the data analysis are described in the next section. The temperature dependence of the MSFs for different atomic classes is discussed in Results and Discussion. The outcome

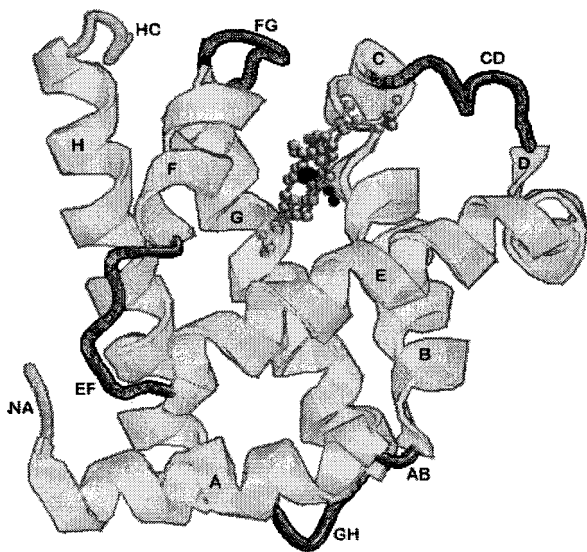


FIGURE 2 Schematic view of carboxy-myoglobin. The protein consists of 153 amino acids, arranged in eight α -helices connected by loops (here represented as wires). The protein structure elements are lettered and defined as follows: amino terminus NA, from amino acid 1 to amino acid 2; helix A, from 3 to 18; corner AB, amino acid 19; helix B, from 20 to 35; helix C, from 36 to 42; loop CD, from 43 to 50; helix D, from 51 to 57; helix E, from 58 to 77; loop EF, from 78 to 85; helix F, from 86 to 94; loop FG, from 95 to 99; helix G, from 100 to 118; loop GH, from 119 to 124; helix H, from 125 to 148; carboxyl terminus HC, from amino acid 149 to amino acid 153. The heavy atoms of the heme group (*dark gray*), the iron atom and the CO molecule (*black*) are also shown, in ball-and-stick representation.

of our simulations is in agreement with experimental findings, in particular for the overall iron motions measured by Mössbauer spectroscopy. Moreover, we obtained insight on the effects of trehalose on the dynamics of protein regions that cannot be experimentally detected.

COMPUTATIONAL METHODS

MD simulations have been performed using the DL-PROTEIN program (Melchionna and Cozzini, 1997). The CHARMM22 force field has been used (MacKerell et al., 1998) with a CHARMM-type parameter set proposed for carbohydrates for trehalose (Ha et al., 1988); the TIP3P model was considered for the water molecules (Jorgensen et al., 1983).

The initial coordinates for the protein were obtained from the crystallographic data of sperm whale myoglobin (Cheng and Schoenborn, 1990). All hydrogen atoms were explicitly included; the protein, consisting of 2543 atoms, was equilibrated at 300 K in vacuo over a 40-ps simulation. A crystalline configuration of trehalose dihydrate (Taga et al., 1972) composed of eight unit cells (32 trehalose and 64 trehalose-bound water molecules) was generated and was equilibrated at 300 K over an 80-ps simulation. The protein was placed into a rectangular cell that was filled with the solvent (trehalose + water molecules), using the pre-equilibrated sugar-water configuration as a building block. Molecules whose atoms were within a 1.8 Å from any protein atom were removed, thus leaving 231 trehalose and 547 H₂O molecules. To ensure the neutrality of the box, nine water molecules were then replaced by nine chlorine counterions, leaving an 89% (w/w) trehalose-water ratio. A system with such a water-trehalose ratio is in a glassy state at room temperature (Green and Angell, 1989).

It is worth noting here that even in an MbCO-trehalose sample exhaustively dried under nitrogen atmosphere at room temperature, an average of two water molecules per trehalose molecule is present (Librizzi et al., 1999b). Moreover, the inhibition of the protein's internal dynamics, as shown by the thermal interconversion among MbCO A substates, is largely dependent on the amount of residual water present in nonexhaustively dried MbCO-trehalose samples (Librizzi et al., 1999b, and work in progress). Our water-sugar ratio, therefore, refers to a system not extremely dry, where some localized substate interconversion can take place (Librizzi et al., 1999a, and work in progress).

The system was equilibrated at 300 K over 110 ps at constant volume and temperature, by coupling with a Nosé thermostat with a time constant of 0.4 ps (Nosé, 1984). A 70-ps simulation was further performed at constant pressure ($P = 1$ kbar) and temperature ($T = 300$ K) by using the Nosé-Hoover technique (Melchionna and Ciccotti, 1997). The coupling constants used were 0.5 ps and 5 ps for the thermostat and the barostat, respectively. This led to a final system density of 1.4 gr/cm³, in agreement with simulated (Conrad and de Pablo, 1999) and experimental (Magazù et al., 1997) data on trehalose-water systems.

The simulation for data collection was performed in the microcanonical ensemble and consisted of a 300-ps trajectory at a temperature of 302 ± 2 K. At the end of the simulation the root-mean-square deviation from the protein's crystal structure thermalized at 300 K in vacuo was 2.4 Å for all the protein atoms, 1.8 Å for the backbone atoms, and 2.2 Å for the heme atoms.

For temperatures below 300 K, equilibration runs were performed in the canonical ensemble. Each equilibration started from the last configuration obtained in the preceding run at higher temperature. The following simulations for data collection were performed in the microcanonical ensemble: 1) a 180-ps trajectory at 277 ± 2 K; and 2) three 100-ps trajectories at 215 ± 1 K, 163 ± 1 K, and 104 ± 1 K, respectively.

Periodic boundary conditions were used (Allen and Tildesley, 1987); van der Waals interactions have been cut off beyond a distance of 10 Å. Electrostatic interactions were calculated by the Ewald sum using the PME method (Essmann et al., 1995); the direct sum cutoff was 10 Å, the Ewald α parameter was set to 0.32, and eight order cubic spline interpolation with

a grid of 40*50*40 points was used. All chemical bonds were kept fixed by using the SHAKE constraint algorithm (Ryckaert et al., 1977; Ciccotti and Ryckaert, 1986). The equations of motion were integrated with the Velocity Verlet scheme (Andersen, 1983; Martyna et al., 1996), with a step size of 1 fs. Coordinate sets were saved every 200 fs for data analysis.

Each configuration $\{r_i, i = 1, N\}$ was best-fitted to the framework of the starting structure in order to correct for the effects due to possible rigid translations and rotations of the protein (Kneller, 1991). Letting the new configuration $\{r_i^*, i = 1, N\}$, the MSFs were calculated from the reconstructed configurations as the following isotropic average:

$$\frac{1}{3} [(\langle x_i^{*2} \rangle - \langle x_i^{*2} \rangle) + (\langle y_i^{*2} \rangle - \langle y_i^{*2} \rangle) + (\langle z_i^{*2} \rangle - \langle z_i^{*2} \rangle)]$$

$$i = 1, N$$

in which the angular brackets indicate time averages.

All the simulations on the H₂O system (Venturoli, 1998) have been performed by using the DL-PROTEIN program (Melchionna and Cozzini, 1997). The system consisted of a MbCO embedded in 1513 water molecules plus nine chlorine counterions; the CHARMM22 (MacKerell et al., 1998) parameter set was used for MbCO, and the TIP3P model (Jorgensen et al., 1983) for water molecules. Simulations have been performed at different temperatures in the 80–300 K range in the isobaric-isothermal ensemble ($P = 1$ bar), by using the Nosé-Hoover technique (Melchionna and Ciccotti, 1997) with time constants of 0.4 ps and 4 ps for the thermostat and the barostat, respectively. Periodic boundary conditions were used (Allen and Tildesley, 1987); van der Waals interactions have been cut off at 12 Å, and electrostatic interactions were computed by using the Ewald sums (Allen and Tildesley, 1987). All chemical bonds were kept fixed by using the SHAKE constraint algorithm (Ryckaert et al., 1977; Ciccotti and Ryckaert, 1986). The equations of motion were integrated with the Velocity Verlet scheme (Andersen, 1983; Martyna et al., 1996), with a step size of 1 fs. The trajectories at different temperatures were propagated in time for different lengths, from 300 ps at the highest temperature to 100 ps at the lowest one; coordinate sets were saved every 200 fs for data analysis.

RESULTS AND DISCUSSION

In Fig. 3 are shown the MSFs, as a function of temperature, relative to 1) all MbCO atoms, 2) side-chain atoms, and 3) backbone atoms. As is evident from data in Fig. 3, the MSFs temperature dependence deviates from the linear behavior at temperatures higher than in simulated H₂O-solvated protein; moreover, this deviation, which reflects the occurrence of the above-mentioned protein-specific motions, is, at all temperatures, of larger extent for hydrated MbCO than for trehalose-coated MbCO. These data are in agreement with experimental results (Cordone et al., 1998, 1999; Librizzi et al., 1999a), and indicate that, in trehalose, substate interconversion is considerably hindered.

Fig. 4 A shows the simulated data for the overall motion of the iron atom of MbCO, both H₂O-solvated and embedded in trehalose; analogous data obtained from Mössbauer spectroscopy (Cordone et al., 1998; Parak et al., 1982) are also reported, for comparison. Data in Fig. 4 A show the agreement between experimental and simulated MSFs in the linear regime (which, in trehalose, extends up to ~270 K). This agreement indicates that the force field used in the

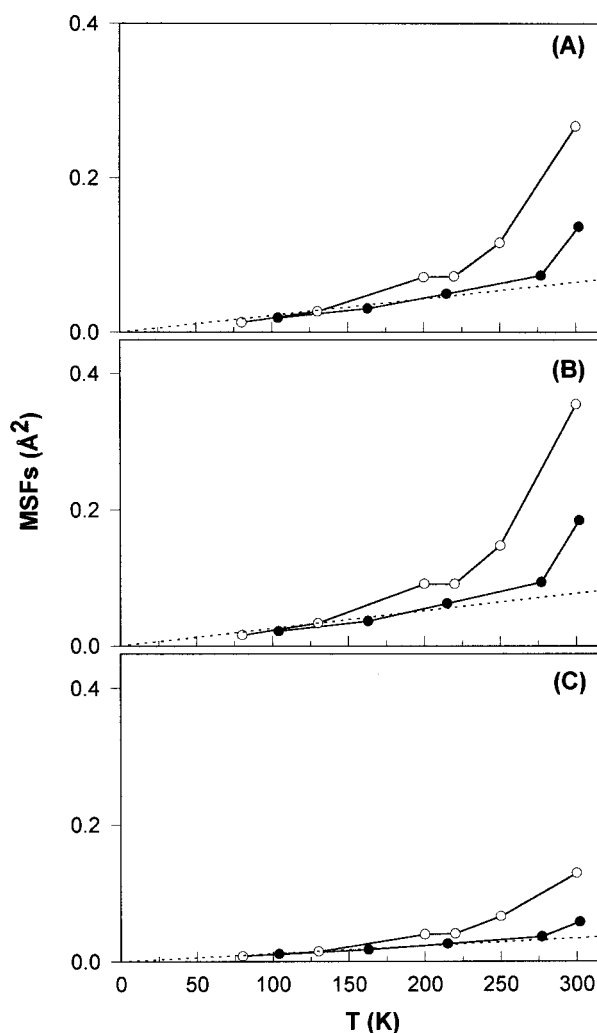


FIGURE 3 Temperature dependence of the MSFs for different atomic classes. (A) All protein atoms; (B) side-chain atoms; (C) backbone atoms. ●, This work; ○, simulated H₂O-solvated MbCO (Venturoli, 1998). The dotted line represents the harmonic behavior extrapolated at 320 K for the trehalose system, obtained by a linear regression on the data points up to 215 K.

simulations well describes the MbCO harmonic behavior both for trehalose-coated and H₂O-solvated protein.

The deviation from the linear behavior for the iron MSFs in H₂O-solvated protein appears at the same temperature as in Mössbauer measurements (Parak et al., 1982). However, above $T \sim 200$ K, the simulations retrieve MSFs lower than the experimental ones, 0.04 Å² and 0.07 Å², respectively, at 300 K; Kuczera et al. (1990), in a simulation of MbCO in vacuo, obtained a value 0.06 Å² for the analogous quantity (at 325 K). The disagreement between experimental and simulated data, attributed by Parak and Knapp (1984) to too short simulation times, cannot be resolved because the time scale of the iron motions probed by Mössbauer spectroscopy ($\sim 10^{-8}$ s) is, in any case, still unattainable.

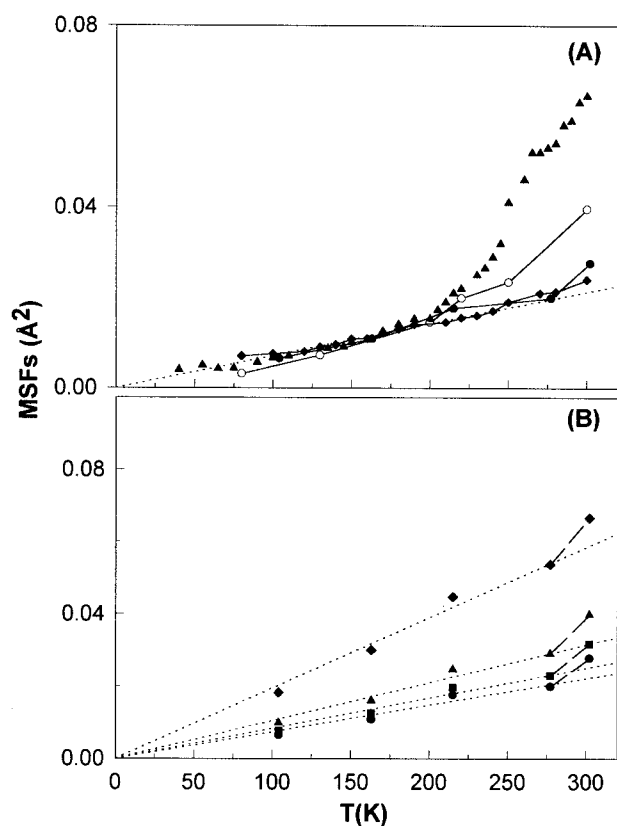


FIGURE 4 Temperature dependence of the MSFs of the iron atom and of the heme heavy atoms. (A) Iron atom: ●, this work; ○, simulated H₂O-solvated MbCO (Venturoli, 1998); ▲ and ◆, data from Mössbauer spectroscopy on deoxy-Mb crystals (Parak et al., 1982) and trehalose-coated MbCO (Cordone et al., 1998), respectively; we recall that the slope of the DW factors versus T is, in myoglobin, independent of the charge and ligation state (Frolov et al., 1997). The dotted line has been drawn with the same slope as the one reported in Cordone et al. (1998) for the experimental Mössbauer data. (B) ●, iron atom; ■, porphyrin nitrogen atoms; ▲, porphyrin heavy atoms; ◆, heavy atoms of the peripheral substituents, this work. The dotted lines represent the harmonic behavior, obtained by a linear regression on the data points up to 277 K, extrapolated at 320 K.

Fig. 4 *B* shows the MSFs, obtained in our simulation, for 1) the nitrogen atoms of the porphyrin ring, 2) all heavy atoms of the porphyrin ring (nitrogen and carbon atoms), and 3) all heavy atoms of the peripheral substituents. Unfortunately, analogous data (except for $T = 300$ K) from the simulation of the H₂O-solvated protein are not available to us. For a better comparison, the MSFs relative to overall iron motion are also reported in Fig. 4 *B*. To show the effects of trehalose we report the values obtained in the

simulations of trehalose-coated and of hydrated MbCO at 300 K in Table 1.

The MSFs shown in Fig. 4 *B* indicate that, in the harmonic regime (up to 277 K), the different subsystems of the heme move within different potential wells. This is shown by the different slopes of the linear harmonic behavior. Instead, the deviation from the linear behavior at 300 K has similar amplitude for all the above subsystems. This suggests that the heme group, including the iron, performs as a whole large-scale motions (called diffusive motions in a limited space or else confined diffusive motions (Parak et al., 1982)), leaving the underlying harmonic vibrations unaltered. This finding agrees with the conclusions recently reported by Parak et al. (1999), who suggested that protein molecules in different conformational substates have similar normal modes, and that normal mode vibrations are still present at room temperature when confined diffusive motions of large portions of the protein take place.

Melchers et al. (1996), on the basis of a normal mode analysis and in agreement with experimental results, showed that the fluctuations of the iron relative to the heme center of mass, for hydrated MbCO, are ~ 30 times lower than those obtained for the overall iron motion. Accordingly, the analogous MSFs resulting from our simulation are reduced by a similar factor at all investigated temperatures; we do not report them here because they are within our statistical noise.

Fig. 5 *A* shows the MSFs, averaged over all the not exchangeable hydrogen atoms, obtained from simulation. As is evident, a large deviation from the linear behavior is present even in the trehalose sample; however, it is smaller than in simulated H₂O-solvated MbCO. In view of the sizeable reduction of the large-scale, confined diffusive motions observed in trehalose, the above deviation from the linear regime is expected not to involve the backbone hydrogen atoms. Rather, it should only involve the more mobile side-chain ones belonging to the external part of residuals. Fig. 5 *B* shows the remarkable difference in mobility between the backbone and the side-chain hydrogen atoms. For the atomic fluctuations of the former our simulation retrieves the same behavior as in neutron scattering (Cordone et al., 1999). We think it is worth mentioning that the above neutron scattering data on trehalose coated MbCO refer to all the hydrogen atoms of the protein and not, as is usual in neutron experiments, to only the not exchangeable ones.

TABLE 1 Room temperature MSFs (in Å²) of the heme heavy atoms

System	Iron Atom	Porphyrin Nitrogen Atoms	Porphyrin Heavy Atoms	Peripheral Substituents Heavy Atoms
MD on trehalose-coated MbCO (this work)	0.027	0.032	0.039	0.067
MD on H ₂ O-solvated MbCO (Venturoli, 1998)	0.039	0.043	0.053	0.123

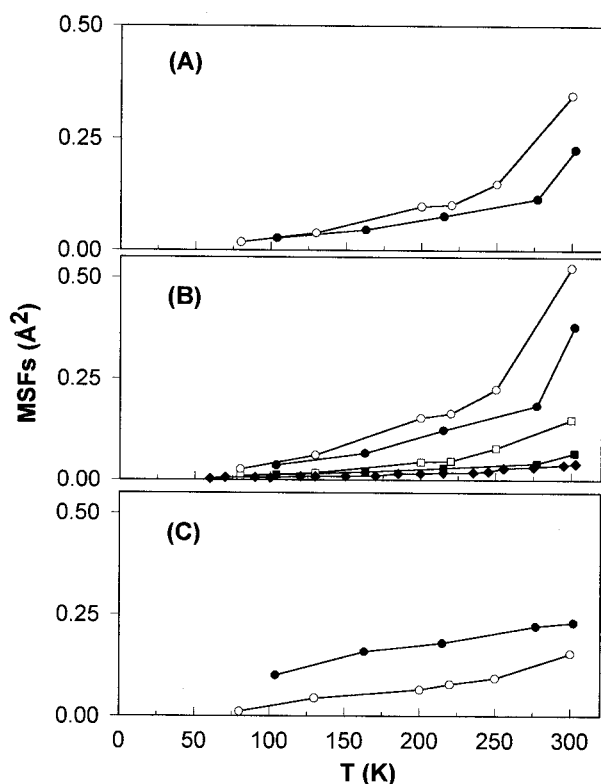


FIGURE 5 Temperature dependence of the MSFs averaged over the nonexchangeable hydrogen atoms. (A) all hydrogen atoms: ●, this work; ○, simulated H₂O-solvated MbCO (Venturoli, 1998). (B) ●, side-chain and ■, backbone hydrogen atoms, this work; ○, side-chain and □, backbone hydrogen atoms, simulated H₂O-solvated MbCO (Venturoli, 1998); ◆, data (all the hydrogen atoms) from neutron diffusion on trehalose-coated MbCO (Cordone et al., 1999). (C) Heme hydrogen atoms: ●, this work; ○, simulated H₂O-solvated MbCO (Venturoli, 1998).

Fig. 5 C shows the MSFs averaged on the heme hydrogen atoms; interestingly, in this case the data obtained from simulation are larger in trehalose than in H₂O-solvated protein at all the temperatures investigated. The fact that these quantities are larger in trehalose even at low temperature suggests that, in the two systems, the heme hydrogen atoms sample different potential surfaces. This, in turn, might be related to different heme configurations.

It is known from experimental results on the kinetics of CO rebinding in MbCO in trehalose glasses (Hagen et al., 1995, 1996) and in sucrose-water solutions (Kleinert et al., 1998; Lichtenegger et al., 1999) that while the CO entry from and release to the outer solvent is blocked (Hagen et al., 1995, 1996) or slowed down (Kleinert et al., 1998), the internal binding step becomes faster in the sugar-water systems than in the glycerol-water solutions (Post et al., 1993). Our simulations indicate at the same time that although, in general, large-scale motions of the protein are considerably reduced in the presence of the sugar matrix, the heme hydrogen atoms have a greater mobility than in the protein-water system. This result therefore might explain

the above experimental findings, by ascribing some specific function in the rebinding kinetics to the motion of the heme hydrogen atoms, as, e.g., in the domed-to-planar heme transition. This phenomenology has been also explained, with a different theoretical approach, in the work of Sastry and Agmon (1997).

Fig. 6 shows the MSFs averaged over all the atoms of the loops CD (from amino acid 43 to amino acid 50) and EF (from 78 to 85) and of the helix C (from 36 to 42), D (from 51 to 57), E (from 58 to 77), and F (from 86 to 94). Again,

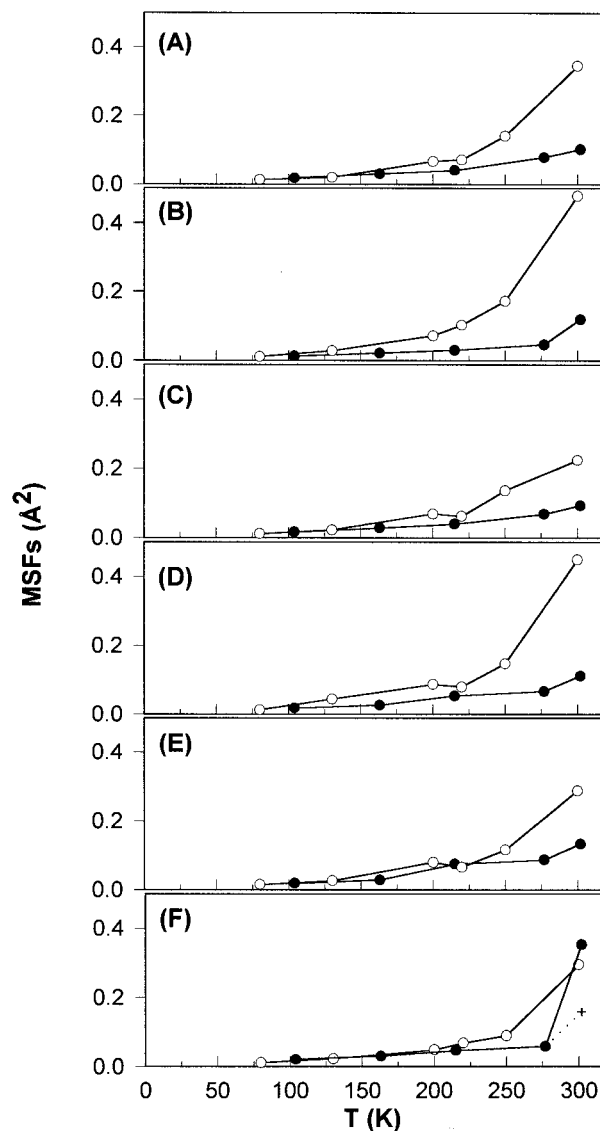


FIGURE 6 Temperature dependence of the MSFs averaged over loops and helix atoms. ●, This work; ○, simulated H₂O-solvated MbCO (Venturoli, 1998). The secondary structure elements are defined as follows: (A) loop CD (from amino acid 43 to amino acid 50); (B) loop EF (from 78 to 85); (C) helix C (from 36 to 42); (D) helix D (from 51 to 57); (E) helix E (from 58 to 77); (F) helix F (from 86 to 94). The cross in panel F represents the 300 K DW factor obtained by averaging on the time interval 30–180 ps in which no jumps appear in the time series shown in Fig. 7.

the trehalose system shows, in general, lower mobility than the H₂O-solvated protein. Analogous behavior is obtained for the other loops and helices present in myoglobin (data not reported). Data in Fig. 6 fully agree with the data relative to the backbone motions (see Fig. 3 C), and confirm that the sugar largely hinders the large-scale functional motions involved in CO diffusion within the protein. The rather large MSFs at 300 K evident for the (otherwise extremely rigid) F helix (see Fig. 6 F), can be rationalized by analyzing the time series shown in Fig. 7. These time series refer to the position of the atoms of the methylene group in position 3 of the amino acid proline 88 (which belongs to the F helix), for both the trehalose and H₂O-solvated system. As Fig. 7 shows, the fluctuations of the atomic motions are largely reduced in the trehalose sample; however, several step transitions occur along the 300-ps trajectory at 300 K in the trehalose system, which corresponds to rapid jumps of the atoms between different positions.

This behavior reflects the occurrence of conformational interconversions (Ichiye and Karplus, 1987) that give the main contribution to the MSFs averaged on all the atoms of the F helix, calculated by time averaging on the whole 300-ps trajectory. In Fig. 6 F we also report the MSFs obtained by time-averaging only in the window 30–180 ps,

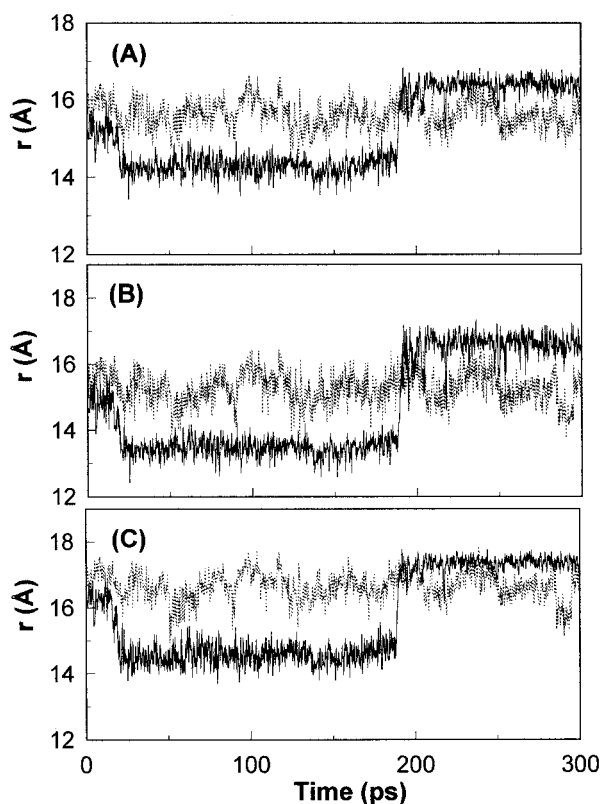


FIGURE 7 Time series of the position of the atoms belonging to the methylene group in position 3 of the amino acid proline 88. (A) carbon atom; (B) and (C) hydrogen atoms. Dark gray: this work; light gray: simulated H₂O-solvated MbCO (Venturoli, 1998).

i.e., within a time interval in which, according to Fig. 7, no conformational transition takes place. As is evident, the resulting amplitude of MSFs agrees with the one shown for the other helices and loops.

CONCLUSIONS

The reported MD simulation on MbCO embedded in a trehalose-water matrix indicates that the so-called protein-specific motions are considerably hindered for almost all atomic classes. This result is in line with recent MD simulation data on an MbCO-water system (Vitkup et al., 2000), with water molecules kept at a lower temperature with respect to the protein to mimic a “high viscosity” solvent.

Moreover, we have been able to characterize the behavior of the system by quantities not always experimentally observable:

1. In the harmonic regime, the different regions of the heme move within different potential wells. This is shown by the temperature dependence of the MSFs of the heme heavy atoms up to 270 K; however, at least in trehalose, at 300 K the heme, including the iron, performs as a whole confined diffusive motions, leaving the underlying harmonic motions unchanged. As mentioned above, this result fully agrees with recent findings reported by Parak et al. (1999);
2. In trehalose, the MSFs of the heme hydrogen atoms exhibit a larger amplitude than in the H₂O-protein system at all the temperatures investigated. This suggests that in trehalose the heme might assume a different configuration with respect to the water-protein system. Furthermore, this result might explain the findings from flash photolysis experiments on MbCO trehalose-coated (Hagen et al., 1995, 1996) and in sucrose-water solutions (Kleinert et al., 1998; Lichtenegger et al., 1999), according to which the ligand rebinding kinetics become faster in trehalose with respect to aqueous solutions (Post et al., 1993);
3. The motional freedom of the loop and helix structures is largely reduced in trehalose with respect to the H₂O-solvated protein. Loop structures are the most flexible regions in the protein (Elber and Karplus, 1987), which mostly regulate the large-scale, confined diffusive motions needed for the protein function, and in particular for ligand diffusion. The above lack of confined diffusive motions is in line with the analogous finding relative to the overall iron motion. Moreover, it agrees with the experimental finding that, for MbCO embedded in a trehalose glass, the CO molecule does not escape from the protein at room temperature even following prolonged illumination (Hagen et al., 1995, 1996; Gottfried et al., 1996). This finding has been found to hold true also in most humid MbCO trehalose samples or in dry samples re-humidified overnight in the presence of 75% relative humidity (Librizzi et al., 1999b).

We thank M. Venturoli and S. Melchionna for providing the simulated data on the H₂O-solvated protein, F. Librizzi and E. Vitrano for permitting quotation of unpublished data and for useful discussions, and A. Cupane and M. Leone for useful discussions.

This work is part of a project co-financed by MURST and European Community (European Funds for Regional Development).

REFERENCES

- Allen, M. P., and D. J. Tildesley. 1987. *Computer Simulation of Liquids*. Clarendon Press, Oxford.
- Andersen, H. C. 1983. RATTLE: a "velocity" version of the SHAKE algorithm for molecular dynamics calculations. *J. Comput. Phys.* 52: 24–34.
- Bianchi, G., A. Gamba, C. Murellie, F. Salamini, and D. Bartels. 1991. Novel carbohydrate metabolism in the resurrection plant, *Craterostigma plantagineum*. *Plant J.* 1:355–359.
- Bonanno, G., R. Noto, and S. L. Fornili. 1998. Water interaction with α,α -trehalose: molecular dynamics simulation. *J. Chem. Soc., Faraday Trans.* 94:2755–2762.
- Cheng, X., and B. P. Schoenborn. 1990. Hydration in protein crystals. A neutron diffraction analysis of carbonmonoxymyoglobin. *Acta Crystallogr.* B46:195.
- Ciccotti, G., and J. P. Ryckaert. 1986. Molecular dynamics simulations of rigid molecules. *Comp. Phys. Rep.* 4:345–392.
- Conrad, P. B., and J. J. de Pablo. 1999. Computer simulation of the cryoprotectant disaccharide α,α -trehalose in aqueous solution. *J. Phys. Chem. A.* 103:4049–4055.
- Cordone, L., M. Ferrand, E. Vitrano, and G. Zaccai. 1999. Harmonic behavior of trehalose-coated carbon-monoxymyoglobin at high temperature. *Biophys. J.* 76:1043–1047.
- Cordone, L., P. Galajda, E. Vitrano, A. Gassmann, A. Ostermann, and F. Parak. 1998. A reduction of protein specific motions in co-ligated myoglobin embedded in a trehalose glass. *Eur. Biophys. J.* 27:173–176.
- Crowe, J. H., and L. M. Crowe. 1984. Preservation of membranes in anhydrobiotic organisms: the role of trehalose. *Science.* 223:701–703.
- Crowe, L. M., S. R. David, and J. H. Crowe. 1996. Is trehalose special for preserving dry biomaterials? *Biophys. J.* 71:2087–2093.
- Doster, W., S. Cusak, and W. Petry. 1989. Dynamical transition of myoglobin revealed by inelastic neutron scattering. *Nature.* 337:754–756.
- Elber, R., and M. Karplus. 1987. Multiple conformational states of proteins: a molecular dynamics analysis of myoglobin. *Science.* 235: 318–321.
- Essmann, U., L. Perera, M. Berkowitz, T. Darden, H. Lee, and L. G. Pedersen. 1995. A smooth particle mesh Ewald method. *J. Chem. Phys.* 103:8577–8593.
- Frauenfelder, H., F. Parak, and R. D. Young. 1988. Conformational substates in proteins. *Annu. Rev. Biophys. Chem.* 17:451–479.
- Frolov, E. N., R. Gvosdev, V. I. Goldanskii, and F. Parak. 1997. Differences in the dynamics of oxidized and reduced cytochrome c measured by Mossbauer spectroscopy. *J. Bio. Inorg. Chem.* 2:710–713.
- Gottfried, D. S., E. S. Peterson, A. G. Sheikh, J. Wang, M. Yang, and J. M. Friedman. 1996. Evidence for damped hemoglobin dynamics in a room temperature glass. *J. Phys. Chem.* 100:12034–12042.
- Green, J., and C. A. Angell. 1989. Phase relations and vitrification in saccharide-water solutions and the trehalose anomaly. *J. Phys. Chem.* 93:2880–2882.
- Ha, A. S. N., A. Giammona, M. Field, and J. W. Brady. 1988. A revised potential energy surface for molecular mechanics studies of carbohydrates. *Carbohydrate Res.* 180:207–221.
- Hagen, S. J., J. Hofrichter, and W. A. Eaton. 1995. Protein reaction kinetics in a room temperature glass. *Science.* 269:959–962.
- Hagen, S. J., J. Hofrichter, and W. A. Eaton. 1996. Geminate rebinding and conformational dynamics of myoglobin embedded in a glass at room temperature. *J. Phys. Chem.* 100:12008–12021.
- Ichiye, T., and M. Karplus. 1987. Anisotropy and anharmonicity of atomic fluctuations in proteins: analysis of a molecular dynamics simulation. *Proteins.* 2:236–259.
- Jorgensen, W. L., J. Chandrasekhar, J. D. Madura, R. W. Impey, and M. L. Klein. 1983. Comparison of simple potential functions for simulating liquid water. *J. Chem. Phys.* 79:926–935.
- Kleinert, T., W. Doster, H. Leysner, W. Petry, V. Schwarz, and M. Settles. 1998. Solvent composition and viscosity effects on the kinetics of CO binding to horse myoglobin. *Biochemistry.* 37:717–733.
- Kneller, G. R. 1991. Superposition of molecular structures using quaternions. *Mol. Sim.* 7:113–119.
- Kuczera, K., J. Kuryan, and M. Karplus. 1990. Temperature dependence of the structure and dynamics of myoglobin. *J. Mol. Biol.* 213:351–373.
- Librizzi, F., E. Vitrano, and L. Cordone. 1999a. Inhibition of A substates interconversion in trehalose coated carbonmonoxymyoglobin. In *Biological Physics*. H. Frauenfelder, G. Hummer, and R. Garcia, editors. AIP American Institute of Physics, Melville, New York. 132–138.
- Librizzi, F., E. Vitrano, and L. Cordone. 1999b. Dehydration and crystallization of trehalose and sucrose glasses containing carbonmonoxymyoglobin. *Biophys. J.* 76:2727–2734.
- Lichtenegger, H., W. Doster, T. Kleinert, A. Birk, B. Sepiol, and G. Vogl. 1999. Heme-solvent coupling: a Mössbauer study of myoglobin in sucrose. *Biophys. J.* 76:414–422.
- Liu, Q., R. K. Schmidt, B. Teo, P. A. Karplus, and J. W. Brady. 1997. Molecular dynamics studies of the hydration of α,α -trehalose. *J. Am. Chem. Soc.* 119:7851–7862.
- MacKerell, A. D., Jr., D. Bashford, M. Bellott, R. L. Dunbrack, Jr., J. D. Evanseck, M. J. Field, S. Fischer, J. Gao, H. Guo, S. Ha, D. Joseph-McCarthy, L. Kuchnir, K. Kuczera, F. T. K. Lau, C. Mattos, S. Michnick, T. Ngo, D. T. Nguyen, B. Prodhom, W. E. Reiher III, B. Roux, M. Schlenkrich, J. C. Smith, R. Stote, J. Straub, M. Watanabe, J. Wiórkiewicz-Kuczera, D. Yin, and M. Karplus. 1998. All-atom empirical potential for molecular modeling in dynamics studies of proteins. *J. Phys. Chem. B.* 102:3586–3616.
- Magazù, S., P. Migliardo, A. M. Musolino, and M. T. Sciortino. 1997. α,α -Trehalose-water solutions. I. Hydration phenomena and anomalies in the acoustic properties. *J. Phys. Chem. B.* 101:2348–2351.
- Makinen, M. W., R. A. Houtchens, and W. S. Caughey. 1979. Structure of carboxymyoglobin in crystals and in solutions. *Proc. Natl. Acad. Sci. U.S.A.* 76:6042–6046.
- Martyna, G. J., M. E. Tuckerman, D. J. Tobias, and M. L. Klein. 1996. Explicit reversible integrators for extended systems dynamics. *Mol. Phys.* 87:1117–1157.
- Mayer, E. 1994. FTIR spectroscopic study of the dynamics of conformational substates in hydrated carbonyl-myoglobin films via temperature dependence of the CO stretching band parameters. *Biophys. J.* 67: 862–873.
- Melchers, B., E. W. Knapp, F. Parak, L. Cordone, A. Cupane, and M. Leone. 1996. Structural fluctuations of myoglobin from normal-modes, Mossbauer, Raman, and absorption spectroscopy. *Biophys. J.* 70: 2092–2099.
- Melchionna, S., and G. Ciccotti. 1997. Atomic stress isobaric scaling for systems subjected to holonomic constraints. *J. Chem. Phys.* 106: 195–199.
- Melchionna, S., and S. Cazzini. 1997. DL_PROTEIN 1.2 User Manual. DL_PROTEIN has been developed from DL_POLY for the simulation of proteins by the Istituto Nazionale di Fisica della Materia, under the Network on "MD simulation of biosystems," group University of Rome La Sapienza. DL_POLY is a package of molecular simulation routines written by W. Smith and T. R. Forrester, copyright The Council for Central Laboratory of the Research Councils, Daresbury Laboratory at Daresbury, Nr. Warrington, UK (1996).
- Nosé, S. 1984. A molecular dynamics method for simulations in the canonical ensemble. *Mol. Phys.* 52:255–268.
- Panek, A. D. 1995. Trehalose metabolism - new horizons in technological applications. *Braz. J. Med. Biol. Res.* 28:169–181.
- Parak, F., and E. W. Knapp. 1984. A consistent picture of protein dynamics. *Proc. Natl. Acad. U.S.A.* 81:7088–7091.

- Parak, F., E. W. Knapp, and D. Kucheida. 1982. Protein dynamics: Mossbauer spectroscopy on deoxymyoglobin crystals. *J. Mol. Biol.* 161: 177–194.
- Parak, F., A. Ostermann, A. Gassmann, C. Scherk, S. H. Chong, A. Kidera, and N. Go. 1999. Biomolecules: fluctuations and relaxations. In *Biological Physics*. H. Frauenfelder, G. Hummer, and R. Garcia, editors. AIP American Institute of Physics, Melville, New York. 117–127.
- Post, F., W. Doster, G. Karvounis, and M. Settles. 1993. Structural relaxation and nonexponential kinetics of CO-binding to horse myoglobin. *Biophys. J.* 64:1833–1842.
- Ryckaert, J. P., G. Ciccotti, and H. J. C. Berendsen. 1977. Numerical integration of the Cartesian equations of motion of a system with constraints: molecular dynamics of n-alkanes. *J. Comp. Phys.* 23: 327–341.
- Sakurai, M., M. Murata, Y. Inoue, A. Hino, and S. Kobayashi. 1997. Molecular-dynamics study of aqueous solution of trehalose and maltose: implication for the biological function of trehalose. *Bull. Chem. Soc. Jpn.* 70:847–858.
- Sastry, G. M., and N. Agmon. 1997. Trehalose prevents myoglobin collapse and preserves its internal mobility. *Biochemistry.* 36:7097–7108.
- Taga, T., M. Senma, and K. Osaki. 1972. The crystal and molecular structure of trehalose dihydrate. *Acta Crystallogr. B.* 29:3258–3263.
- Venturoli, M. 1998. *Dinamica Molecolare della Mioglobina*, Thesis, University of Rome La Sapienza.
- Vitkup, D., D. Ringe, G. A. Petsko, and M. Karplus. 2000. Solvent mobility and the protein “glass” transition. *Nat. Struct. Biol.* 7:34–38.
- Vojtechovsky, J., K. Chu, J. Berendzen, R. M. Sweet, and I. Schlichting. 1999. Crystal structures of myoglobin-ligand complexes at near-atomic resolution. *Biophys. J.* 77:2153–2174.